Surface Composition Control via Chain End Segregation in Blend Films of Polystyrene and Poly(vinyl methyl ether)

Daisuke Kawaguchi, Keiji Tanaka, and Tisato Kajiyama*

Department of Applied Chemistry, Faculty of Engineering, Kyushu University, Fukuoka 812-8581, Japan

Atsushi Takahara

Institute for Fundamental Research of Organic Chemistry, Kyushu University, Fukuoka 812-8581, Japan

Seiji Tasaki

Research Reactor Institute, Kyoto University, Osaka 590-0494, Japan

Received January 28, 2003; Revised Manuscript Received June 24, 2003

ABSTRACT: Surface aggregation states in miscible blends of monodisperse polystyrene (PS) and poly(vinyl methyl ether) (PVME) were studied by X-ray photoelectron spectroscopy (XPS) in conjunction with neutron reflectivity (NR). In the case of symmetric blends in terms of degree of polymerization, N, PVME and PS were preferentially segregated at the film surface and the interface with a silicon wafer, respectively, to minimize free energy of the system. The concentration profile near the surface obtained by experiments was consistent with a mean-field prediction. Also, the surface composition in symmetric blends composed of PS terminated by fluoroalkyl groups at both ends (α,ω-PS$(R_f)_2$) and PVME was examined. In this case, the surface enrichment of PVME was suppressed by virtue of the surface localization of fluoroalkyl end groups, and the composition was strongly dependent on N. The surface in asymmetric α,ω-PS$(R_f)_2$/PVME blend, in which N of α,ω-PS$(R_f)_2$ was much smaller than that of PVME, was mostly covered with the PS segments. The results presented imply a possibility that the surface composition in miscible polymer mixtures could be perfectly regulated combining the chain end effect with the molecular weight disparity between the components.

Introduction

Aggregation states and physical properties at polymeric solid surfaces are often different from those in its interior bulk region.[1−3] For example, it has been widely accepted that in the case of symmetric miscible mixtures of two polymers, a lower surface energy component is enriched at the surface.[4−16] Also, the concentration profile near the surface can be well expressed by mean-field and self-consistent mean-field models.[5−11,13,15,16] This can be simply understood by taking into account thermodynamics at the surface; that is, the lower surface energy component energetically prefers to contact with the zero surface energy medium such as air or vacuum. However, depending on an objective for technological applications of polymeric materials, sometimes the surface segregation of a higher surface energy component in the blends might be desired. Hence, to design and construct highly functionalized polymer surfaces, it is crucially important to explore how the surface peculiarities can be controlled without changing the bulk structure and properties.

As one of other responsible factors determining on the surface segregation phenomena in miscible binary mixtures, molecular weight disparity between the components has been studied experimentally[17,18] and theoretically.[19] Thus far, we have examined the surface composition in mixtures of two polystyrenes (PS) with different molecular weights by scanning force microscopy.[18] As a result, it was elucidated that a smaller molecular weight PS was enriched at the surface and that the inclination became more remarkable with increasing molecular weight difference. In a strict sense, it is still an open question at present why a smaller molecular weight component is preferentially partitioned to the surface. However, it would be accounted for by two factors: flattened chain conformation[20,21] and localization of chain end groups[22−24] at the surface. The first can be understood by considering that a shorter component suffers less of a conformational entropic penalty than a longer one at the surface,[2,17,18] and the second is as though chain ends behave like floating buoys.[25,26] That is, as the number density of chain ends increases, the segments directly connected to the end groups are inevitably pulled out to the surface. Probably, both make the surface free energy of the smaller molecular weight component lower, resulting in surface enrichment of the smaller molecular weight component.

It is of interest to study the surface in a binary blend system, in which a smaller molecular weight component possesses a higher surface energy. In that case, the both effects of surface energy and molecular weight disparity repugnantly act on the surface segregation. So far, such studies have been made using the mixtures of PS and deuterated PS (dPS).[17,18] Even though the surface energy of dPS is slightly lower than that of PS, PS can be enriched at the surface, provided that it is a smaller molecular weight component. This means that it is experimentally possible to enrich a higher surface energy component at the surface in the miscible polymer blends by utilizing the effect of molecular weight disparity. Then, a question arises as to whether this notion is universal over miscible binary mixtures. The surface energy difference between PS and dPS is only 0.08 mJ m^{-1}. If the difference becomes extremely larger, what

* To whom correspondence should be addressed: Fax +81-92-651-5606; Tel +81-92-642-3560; e-mail kajiyama@cstf.kyushu-u.ac.jp.

10.1021/ma034117u CCC: $25.00
Published on Web 08/06/2003

Table 1. Polymers Used in This Study

sample	M_n	$N \times 10^{-3}$	M_w/M_n
dPS	128K	1.14	1.11
	107K	0.96	1.11
	49K	0.44	1.06
	27K	0.24	1.05
α,ω-dPS(R_f)$_2$	157K	1.40	1.11
α,ω-PS(R_f)$_2$	47.8K	0.45	1.18
	25.2K	0.24	1.12
	10.2K	0.09	1.11
PVME	87.7K	1.51	1.19
	77.0K	1.33	1.18
	68.2K	1.18	1.14
	61.2K	1.06	1.12
	28.9K	0.50	1.27
	25.7K	0.44	1.17
	15.0K	0.26	1.28
	12.5K	0.22	1.26

happens with the surface segregation?

A pair of PS and poly(vinyl methyl ether) (PVME) has been widely studied as a complete miscible mixture at room temperature.[27,28] Consequently, it was clearly shown that PVME with the lower surface energy than PS by 7 mJ m^{-2} was preferentially segregated at the surface.[29−35] In this blend system, the surface energy difference between the two components was 88 times larger than that for the PS/dPS blend. Hence, in this study, we focus on the surface in the PS/PVME blend system. At first, the surface segregation in blend films composed of monodisperse PS and fractionated PVME is revisited. This is because details of the segregated structure at the surface, such as surface decay length and excess amount, have not been clarified yet. Then, we present how the chemical composition at the surface in the PS/PVME blend films can be controlled.

Experimental Section

Polymers used in this study were PS, deuterated PS (dPS), PS and dPS terminated at both ends with fluoroalkylsilyl groups (α,ω-PS(R_f)$_2$ and α,ω-dPS(R_f)$_2$) and poly(vinyl methyl ether) (PVME). PS, α,ω-PS(R_f)$_2$, and α,ω-dPS(R_f)$_2$ were synthesized by living anionic polymerizations. For α,ω-PS(R_f)$_2$ and α,ω-dPS(R_f)$_2$, metal naphthalene and (tridecafuluoro-1,1,2,2-tetrahydrooctyl)dimethylchlorosilane were used as an initiator and a terminator, respectively.[24] dPS and PVME were purchased from Polymer Source Inc. and Scientific Polymer Products Inc. Since the purchased PVME without purification possessed a broad molecular weight distribution, it was fractionated by gel permeation chromatography using a Shodex KF-2004 column. Table 1 tabulates number-average molecular weight, M_n, degree of polymerization, N, and polydispersity index, M_w/M_n, where M_w denotes weight-average molecular weight, for the polymers used.

Blends of PVME and PS, dPS, α,ω-PS(R_f)$_2$, or α,ω-dPS(R_f)$_2$ were prepared by mixing each toluene solution and were basically symmetric in terms of N unless it is stated. Also, the mixing ratio of the blends were fixed to be 50 wt %. The blend films were spun-coated from the toluene solutions onto silicon wafers with native oxide layer. The thickness of all blend films evaluated by ellipsometry was approximately 110 nm, which was sufficient to avoid any ultrathinning effects on the surface aggregation states. These films were annealed for 150 h at 333 K, which was well above the bulk glass transition temperature[27,33] and below the lower critical solution temperature (LCST).[27,33]

Surface chemical composition of the blend films was examined by X-ray photoelectron spectroscopy (XPS). The XPS spectra were obtained with a PHI ESCA 5800 X-ray photoelectron spectrometer (Physical Electronics Co. Ltd.). The X-ray source was Mg Kα X-ray operated at 14 kV and 30 mA. All C_{1s} peaks corresponding to neutral carbon were calibrated at the binding energy for 285.0 eV to correct for the charging

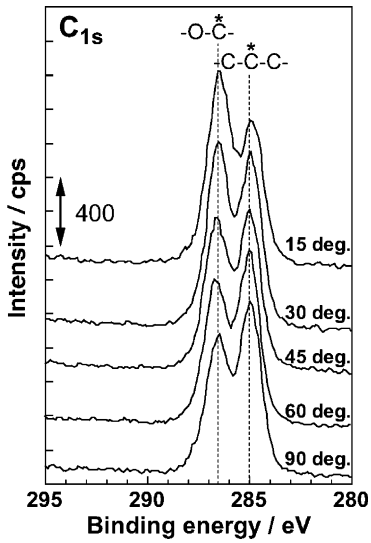

Figure 1. XPS C_{1s} core-level spectra for symmetric dPS-128K/PVME-68.2K (N_{dPS} = 1140, N_{PVME} = 1180) blend film as a function of emission angle of photoelectrons.

energy shift. The analytical depth of XPS, d, from the outermost surface is given by

$$d = 3\lambda \sin\theta \quad (1)$$

where λ and θ are inelastic mean-free path and emission angle of photoelectrons, respectively.[36] According to Ashley's equation, λ for C_{1s} and F_{1s} were estimated to be 3.1 and 2.1 nm, respectively.[37] In the measurement, θ was varied from 15° to 90°.

Neutron reflectivity (NR) measurement was carried out using the multilayer interferometer for neutrons (C3-1-2-2, MINE)[38] at the Institute for Solid State Physics, the University of Tokyo. Incident neutrons have a wavelength, λ_N, of 0.88 nm and a resolution of 5.1%. The reflectivity was calculated on the basis of the scattering length density profile along the depth direction by using Spreadsheet Environmental Reflectivity Fitting.[39]

Results and Discussion

Surface composition in PS/PVME blend system was first studied by Pan and Prest using XPS in 1985.[29] At that time, they used polydisperse PVME. Also, PVME with a broad molecular weight distribution has been used for following studies related to the surface segregation phenomena in the PS/PVME blends.[30−35] Since we have been now aware that a lower molecular weight component is generally enriched at the surface,[17−19] the surface composition of the PS/PVME, in which PVME was fractionated, was revisited at first in this study using XPS and NR. Figure 1 shows the XPS C_{1s} spectra of symmetric dPS-128K/PVME-68.2K (N_{dPS} = 1140, N_{PVME} = 1180) blend film collected at various θ. Here, the usage of *symmetric* means that N values for the both components are almost the same. Also, dPS was used instead of PS so that the surface composition in the blend films obtained by the both techniques of XPS and NR can be directly compared later. Two peaks overlapped in the spectra, and each peak observed at 285.0 and 286.5 eV corresponded to neutral and ether carbons, respectively. Photoelectron intensities of the neutral and the ether carbons decreased and increased with decreasing θ, respectively. Since the ether carbons are only present in PVME, Figure 1 qualitatively indicates that the PVME component is segregated to the surface. The surface composition in the blend films can be extracted

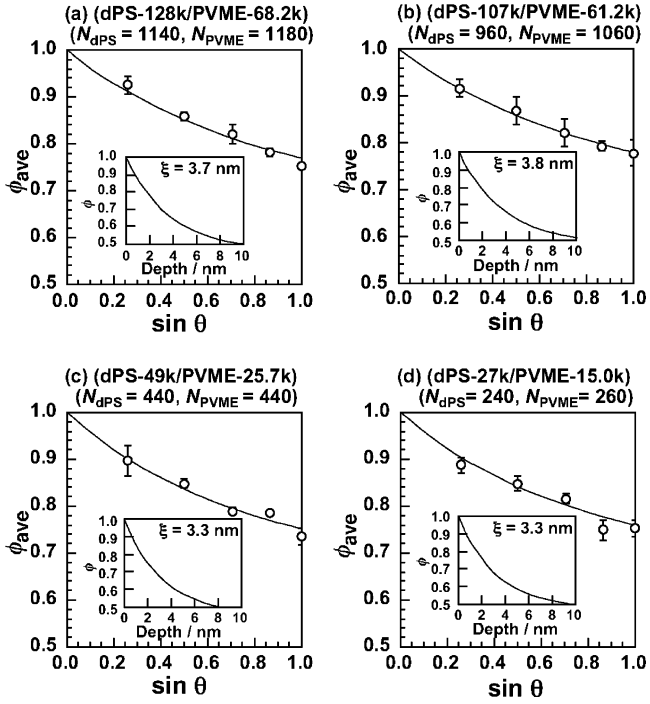

Figure 2. Sin θ dependence of average PVME volume fraction for symmetric dPS/PVME blend films with different M_n pairs. The abscissa of sin θ corresponds to the analytical depth. Open circles are the experimental data, and solid curves in the main panels denote the best-fit ones. The insets show real composition profile in the surface region deduced by a mean-field approximation using the XPS data.

deconvoluting the spectra into two contributions, e.g., neutral and ether carbons, as follows:

$$\frac{I_{CO}}{I_{total}} = \frac{2\phi_{ave}\rho_{VME}/M_{VME}}{3\phi_{ave}\rho_{VME}/M_{VME} + 8(1-\phi_{ave})\rho_{dSt}/M_{dSt}} \quad (2)$$

where ϕ_{ave} is average volume fraction of PVME within a given analytical depth. M_{dSt} and M_{VME} are molecular weights of the repeating units for deuterated styrene and vinyl methyl ether, respectively. Also, ρ_{dSt} and ρ_{VME} are mass densities of dPS and PVME.

Figure 2 shows the surface composition in dPS/PVME blend films with various M_n pairs as a function of sin θ, corresponding to analytical depth. Each inset depicts the corrected composition profile in the surface region down to 10 nm. For all films studied, ϕ_{ave} increased with decreasing sin θ, meaning that the PVME component was gradually enriched toward the surface. However, the inclination was not so sensitive to M_n namely, N, as long as the blends were symmetric.

In general, photoelectrons cannot travel for a long distance in a solid due to inelastic scattering. This means that only photoelectrons emitted from the region in close proximity to the surface can get out of the solid, resulting in the surface sensitivity of the XPS technique. The photoelectron intensity for j-core level at θ is expressed as

$$I_j(\theta) = Fk\int_0^\infty n_j(z)\exp\left\{\frac{-z}{\lambda_j \sin\theta}\right\} dz \quad (3)$$

where z and $n_j(z)$ represent depth and atomic composition−depth profile, respectively. F and k are the transmission function and a factor related to sensitivity. Hence, even though the sampling depth is z, photoelectrons are not uniformly emitted from the depth region from the surface to z. Instead, the detected amount of photoelectrons exponentially decays with increasing depth to z. This means that the dependence of surface composition on sin θ cannot be simply regarded as the compositional depth profile. Thus, the following treatment was made to extract the real composition profile near the surface. Schmidt and Binder, using a mean-field approximation, proposed that the surface composition profile in a miscible polymer blend can be given by[5]

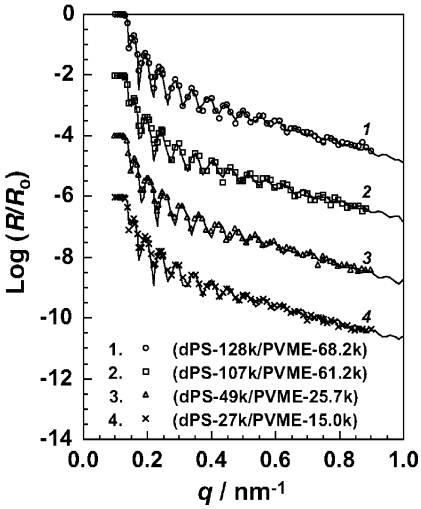

Figure 3. Neutron reflectivity profiles for symmetric dPS/PVME blend films with different M_n pairs. Experimental data sets are shown by symbols. Solid curves depict the best-fit ones calculated from model scattering length density profiles, which are shown in the inset of Figure 4. Experimental data and solid curves are vertically offset for clarity.

$$\phi(z) = \phi_\infty + (\phi_s - \phi_\infty)\exp(-z/\xi) \quad (4)$$

where ϕ_s and ϕ_∞ are surface ($z = 0$) and bulk volume fraction of a component, respectively, and ξ is decay length showing how the surface composition reaches the bulk value. Thus, the composition by XPS at a given θ can be expressed by

$$\phi_{ave}(\theta) = \int_0^\infty \phi(z)\exp\left\{\frac{-z}{\lambda \sin\theta}\right\} dz \quad (5)$$

In this study, ϕ_s and ξ in eq 4 were arbitrarily changed, and ϕ_∞ was set to the mixing ratio. And then, the ϕ_{ave}−sin θ curve was calculated on the basis of eq 5. The solid curves in the main panels of Figure 2 denote the best-fit ones to the experimental data. The insets show the $\phi(z)$ for the best-fit curves and should correspond to the real composition profiles near the surface. For all cases employed, ϕ_s was estimated to be 1.0, and ξ became slightly larger with increasing N. Thus, it seems most likely that the outermost surface of the dPS/PVME blend films was completely covered with PVME being independent of N.

A concentration profile normal to the surface in blend films can be directly examined by NR measurement as well. The NR measurement enables us to gain direct information about the overall concentration profile through the dPS/PVME film,[40,41] meaning that it is also possible to discuss about how the concentration varies in the vicinity of the interface with the substrate. Figure 3 shows the scattering vector, q [= $(4\pi/\lambda_N)$ sin θ_N],

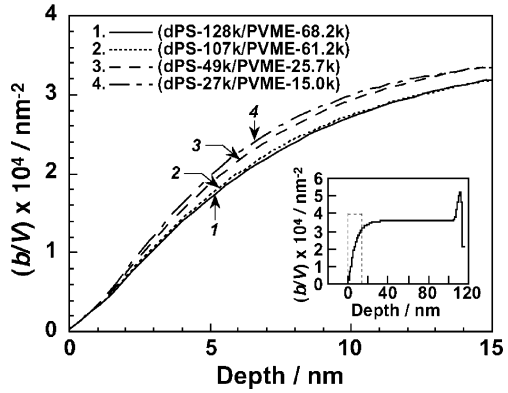

Figure 4. Enlarged scattering length density profiles near the surface region for symmetric dPS/PVME blend films. The inset figure shows the whole profile of dPS-128K/PVME-68.2K blend film as a typical example.

dependence of neutron reflectivity for the dPS/PVME blend films with the same M_n pairs as those for the XPS measurements. Each film thickness was fixed to be about 110 nm. The data for the dPS/PVME films are offset by 2 decades for the sake of clarity. The solid curves denote the best-fit calculated reflectivity to the experimental data based on the model scattering length density (b/V) profiles, as shown in the inset of Figure 4. The (b/V) profiles were basically drawn on the basis of eq 4 in a similar way as the XPS measurements. Since the calculated curves are in good agreement with the experimental data, it can be claimed that the model (b/V) profiles well reflect the compositional changes in the blend films along normal to the surface. For dPS and PVME, the (b/V) values of 6.46×10^{-4} and 3.40×10^{-5} nm^{-2} were used, respectively. Hence, the composition at a given depth was deduced from the (b/V) value at the corresponding depth. The PVME fraction exponentially decayed with increasing depth in the surface region and eventually reached the bulk value, whereas dPS was enriched at the polymer/substrate interface. This result can be simply explained in terms of minimization of free energy at the both of surface and interface. That is, the lower and higher surface energy components energetically prefer to contact with the hydrophobic air or vacuum and the hydrophilic silicon wafer with native oxide layer, respectively.

Lee and Sung also studied surface and interfacial compositions in the PS/PVME blend films prepared on quartz disks by UV reflection spectroscopy[34] and concluded that the PVME component was enriched at the polymer−quartz interface as well as the surface. Although our result related to the interfacial composition is inconsistent with what they observed, it is hard at the moment to identify why the discrepancy was observed in the two experiments because they used polydisperse samples and the blend films with a thickness much thinner than ours such as 30−50 nm. If their PVME contains much shorter chains, they should be entropically driven to the substrate interface.[17−19] And, in the case of ultrathin blend films, the surface and interfacial structure should be perturbed with each other.[42,43] This might be the case for their thickness region. Besides, it may be possible that chemical nature at the surface of their quartz disks differs from that of our silicon wafers with native oxide layer.

We now turn to a comparison of our data with the prediction by a mean-field approximation. According to Schmidt and Binder, the concentration profile near the surface can be expressed by eq 4.[5] Hence, the ϕ_s and ξ values for the current blend system should be anticipated at first. For a symmetric miscible blend, ϕ_s can be estimated from

$$\phi_s = \frac{\phi_\infty + t}{1 + t} \tag{6}$$

where t is a parameter related to surface energy difference between the components, $\Delta\gamma$, and to Flory−Huggins interaction parameter, χ. Here, t is given by

$$t = \left(\frac{3b^3\Delta\gamma}{ak_BT}\right)^2 \frac{1}{\Delta\chi} \tag{7}$$

where b^3 is the volume of a Flory−Huggins lattice site, a is the statistical step length, k_B is the Boltzmann constant, T is the absolute temperature, and $\Delta\chi = \chi_b - \chi$. For the blends, the b^3 and a values were taken to be averaged for PS and PVME: $b^3_{PS} = 1.41 \times 10^{-1}$ nm^3, $b^3_{PVME} = 7.87 \times 10^{-2}$ nm^3;[44] $a_{PS} = 0.68$ nm,[45] $a_{PVME} = 0.69$ nm.[46] And, $\Delta\gamma$ is known to be 7 mJ m^{-2}.[30] Also, χ_b was introduced by Jones and Kramer as χ on the coexistence curve, which can be given by the expression[10]

$$\chi_b = \frac{1}{N(1 - 2\phi_\infty)} \ln\left(\frac{1 - \phi_\infty}{\phi_\infty}\right) \tag{8}$$

Besides, ξ should be equal to the correlation length for bulk concentration fluctuations and is given by[2]

$$\xi = \frac{a}{6}\Big/\left(\frac{1}{2N} - \chi\phi_\infty(1 - \phi_\infty)\right)^{1/2} \tag{9}$$

Here, χ at the annealing temperature of 333 K was deduced to be −2.02 on the basis of small-angle neutron scattering data by Stein and co-workers.[47]

Since the χ_b value could be ignored for the current situation because of $\phi_\infty \sim 0.5$, $\Delta\chi$ and t were supposed to be independent of N. This led to the N independence of ϕ_s. And, t was much larger than ϕ_∞. Hence, ϕ_s was almost unity. This theoretical consideration was in good accordance with the XPS results shown in the insets of Figure 2. Figure 5 shows the N dependence of ξ and z^* for the dPS/PVME blend films obtained by the XPS and NR measurements. Here, z^* is the total excess amount of PVME at the surface and is defined by[2]

$$z^* = \int_0^\infty [\phi(z) - \phi_\infty]\, dz \tag{10}$$

These characteristic values calculated from the aforementioned mean-field theory were also plotted in Figure 5. As a general trend, z^* and ξ slightly increased with increasing N. And, the both z^* and ξ values evaluated by XPS were in good accordance with the predicted values by the mean-field theory. On the other hand, the ξ and z^* values evaluated on the basis of NR were higher than others, although how ξ and z^* increased with increasing N was quite similar to others. A possible explanation of this difference might be correlated to the conditional difference for the both measurements. NR was carried out in an ambient atmosphere, whereas XPS measurement was made under an ultrahigh vacuum. In the ambient atmosphere, PVME absorbs water molecules in the air, and then, the water molecules would diffuse into a surface region of the blend

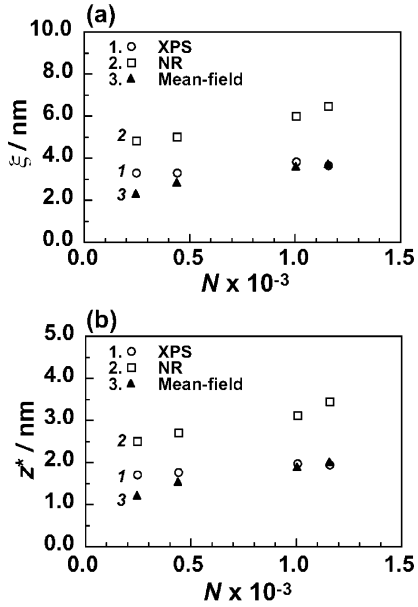

Figure 5. Degree of polymerization dependence of (a) decay length, ξ, and (b) surface excess amount, z^*.

films. If that is the case, (b/V) values in such the region become lower because of a smaller (b/V) value for water molecules.[2] This leads to an exaggeration of the PVME fraction in the surface region as long as the PVME content is calculated under the assumption that the (b/V) value at a given depth is averaged only for dPS and PVME.

We finally come to the surface segregation phenomena in α,ω-PS(R_f)$_2$/PVME blend films. So far, we have studied surface aggregation states in the dPS/PVME blends and reached a conclusion that the lower surface energy component of PVME is enriched at the surface. To control the surface chemical composition, we incorporate an extremely lower surface energy component, fluoroalkyl group, into both ends of PS and then analyze the surface composition in the blend films with PVME. Schacht and Koberstein studied phase behavior of blend systems of PS, in which one end was terminated by the fluoroalkyl group, and PVME based on cloud point curves.[48] In that case, the LCST of the blend increased by 10 K in comparison with before the incorporation of the fluoroalkyl group, resulting in enhanced miscibility. Hence, if the LCST for our blend system alters by the fluoroalkyl end groups, it would increase. Therefore, it seems reasonable to infer that the α,ω-PS(R_f)$_2$/PVME blend systems are also in a miscible state at temperatures employed. Figure 6 shows the analytical depth dependence of surface PVME fraction for the symmetric α,ω-PS(R_f)$_2$/PVME blend films as a function of N. The dotted line denotes the PVME volume fraction in the bulk. In the case of the α,ω-PS(R_f)$_2$-157K/PVME-87.7K and the α,ω-PS(R_f)$_2$-47.8K/PVME-28.9K films, the surface PVME fraction was higher than the bulk value and was invariant with respect to sin θ, implying that there exists a uniform PVME-rich layer in the measured depth region. Also, the surface composition was almost equivalent to the bulk one for the α,ω-PS(R_f)$_2$-25.2K/PVME-12.5K film. That is, no surface enrichment took place for this blend film. These results were inconsistent with the prediction of the composition profile near the surface by eq 4. In other words, the mean-field theory failed for this system.[14] Since the surface PVME fraction decreased with decreasing N, or increasing number

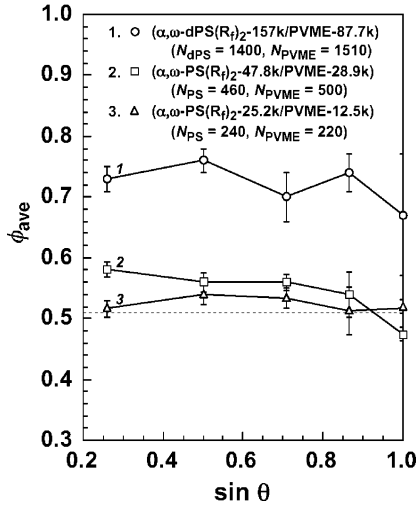

Figure 6. Sin θ dependence of surface PVME fraction for symmetric α,ω-PS(R_f)$_2$/PVME blend films with different M_n pairs.

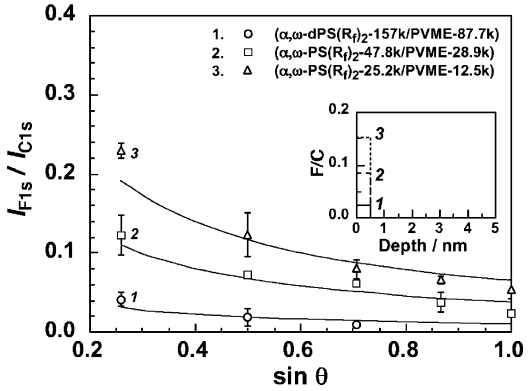

Figure 7. Relation between sin θ and intensity ratio of F_{1s} to C_{1s} for α,ω-PS(R_f)$_2$/PVME blend films with different M_n pairs. Open symbols are the experimental data sets, and solid curves are the best-fit ones calculated on the basis of model depth profiles of (F/C) shown in the inset.

density of R_f chain ends, it is conceivable that the surface enrichment of PVME was suppressed by the presence of R_f chain end groups.

To address R_f chain end distribution near the blend surface, XPS measurement was made. Figure 7 shows the analytical depth dependence of peak intensity ratio of F_{1s} to C_{1s}, I_{F1s}/I_{C1s}, in the α,ω-PS(R_f)$_2$/PVME blend films as a function of N. Since F atom is contained only in the chain end portion, the I_{F1s}/I_{C1s} value can be regarded as an indicator of the chain end concentration. For all α,ω-PS(R_f)$_2$/PVME blend films employed, the I_{F1s}/I_{C1s} value increased with decreasing sin θ. This result clearly indicates that the R_f end groups are preferentially partitioned to the surface. However, the I_{F1s}/I_{C1s} vs sin θ relation cannot be directly referred as the true depth profile, as mentioned above. Hence, the true depth profile was obtained on the basis of Paynter's algorithm.[49] The details have been described elsewhere.[24] The solid curves in Figure 7 depict the best-fit relations of I_{F1s}/I_{C1s} to sin θ using models shown in the inset.[50] On the basis of the inset of Figure 7, it is envisaged that even in the α,ω-PS(R_f)$_2$/PVME blend films, the R_f end groups are almost perfectly localized at the surface due to the lowest surface energy in the system. Since the PS segments are directly connected to the R_f groups, they are inevitably pulled out to the surface. This is as though the chain ends behave like floating buoys for the

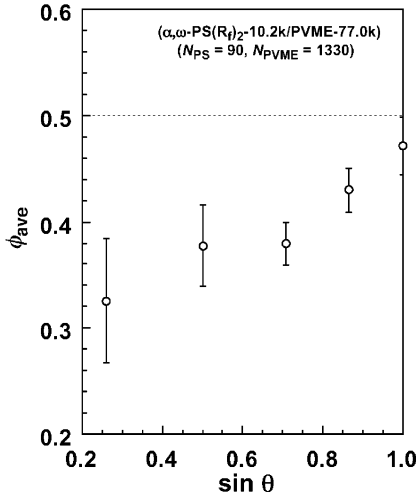

Figure 8. Sin θ dependence of surface PVME fraction for asymmetric α,ω-PS$(R_f)_2$-10.2K/PVME-77.0K blend film.

PS segments. If this notion is correct, to what extent the PVME component is enriched at the surface should be inversely proportional to the number density of the R_f chains ends, namely N. This is actually what was observed in Figure 6. Hence, it seems reasonable to conclude that the PVME fraction at the surface in the α,ω-PS$(R_f)_2$/PVME films was suppressed, owing to the surface localization of the R_f chain ends. The results presented here make it clear that surface chemical composition in polymer blends can be somehow controlled by chain end chemistry of a component.

Although we have seen that chemical modification of the chain ends of PS was quite effective to control the surface composition in the blends, it was not good enough to achieve the surface segregation of the PS component. Hence, an effect of molecular weight disparity between components is combined with chain end chemistry. As stated in the Introduction, a low molecular weight component is generally enriched at the surface[17−19] due probably to the both of conformational entropy loss and localization of chain ends at the surface. Figure 8 shows the relation of sin θ vs surface composition for asymmetric α,ω-PS$(R_f)_2$-10.2K/PVME-77.0K ($N_{PS} = 90$, $N_{PVME} = 1330$) blend film. Interestingly, the PVME fraction decreased with decreasing sin θ, meaning that the PS segments were enriched at the surface and that the concentration asymptotically reached the bulk value with increasing the depth. On the other hand, in the case of asymmetric PS-10.2K/PVME-77.0K film, the surface PVME fraction was still higher than the bulk value, although the extent was also suppressed (not shown). For example, the PVME fraction at sin θ of 0.259 for this blend was about 65 vol %. The difference in the two, α,ω-PS$(R_f)_2$-10.2K/PVME-77.0K and PS-10.2K/PVME-77.0K, was only chain ends of the PS used. Nevertheless, such the chain end effect altered the surface PVME fraction by the factor of approximately 2.

The surface segregation of the PS component could be attained only combining the chain end chemistry with the effect of molecular weight disparity, as shown in Figure 8. Of course, it may be possible that the PS component can be driven to the surface without the chain end chemistry, if the PS component is extremely short. However, such a PS component is no longer polymer and is out of our interests at present. Our results clearly indicate a possibility that surface composition in miscible binary polymer mixtures can be perfectly regulated by chain end chemistry with the aid of molecular weight disparity.

Conclusions

Surface and interfacial aggregation states in symmetric dPS/PVME blend films were studied by XPS in conjunction with NR. It was found that PVME and dPS were enriched at the surface and the interface with silicon wafer, respectively, to minimize interfacial free energy of the system. Also, the concentration profile near the surface and the surface excess amount of the PVME component obtained by experiments were in good agreement with those values anticipated by a mean-field approximation. To control the surface chemical composition in the blends, a lower surface energy component of R_f group was incorporated to both ends of PS and then mixed with PVME. In that case, the surface segregation of the PVME segments was discernibly suppressed on account of the surface localization of the R_f groups. This result tells us that chain end chemistry can be one of the responsible factors for the determination of the surface segregation phenomena in miscible binary polymer blends. Finally, combining the chain end chemistry with molecular weight disparity between the components, it was successfully attained that the PS segments were preferentially segregated at the surface in the blend films.

Acknowledgment. We thank Yasuyuki Yokoe for his help with syntheses of α,ω-PS$(R_f)_2$ and α,ω-dPS$(R_f)_2$. This was in part supported by Grant-in-Aids for Scientific Research (A) (#13355034) and for the 21st century COE program "Functional Innovation of Molecular Informatics" from the Ministry of Education, Culture, Sports, Science and Technology, Japan. Also, this work is partially supported in the utilization of the reactor by the Inter-Univ. Program for common use JAERI facility.

References and Notes

(1) Garbassi, F.; Morra, M.; Occhiello, E. *Polymer Surfaces, from Physics to Technology*; Wiley: Chichester, 1994.
(2) Jones, R. A. L.; Richards, R. W. *Polymers at Surfaces and Interfaces*; Oxford University Press: London, 1995.
(3) Karim, A.; Kumar, S. *Polymer Surfaces, Interfaces and Thin Films*; World Scientific: Singapore, 2000.
(4) Nakanishi, H.; Pincus, P. *J. Chem. Phys.* **1983**, *79*, 997.
(5) Schmidt, I.; Binder, K. *J. Phys. (Paris)* **1985**, *46*, 1631.
(6) Jones, R. A. L.; Kramer, E. J.; Rafailovich, M. H.; Sokolov, J.; Schwarz, S. A. *Phys. Rev. Lett.* **1989**, *62*, 280.
(7) Jones, R. A. L.; Norton, L. J.; Kramer, E. J.; Composto, R. J.; Stein, R. S.; Russell, T. P.; Mansour, A.; Karim, A.; Felcher, G. P.; Rafailovich, M. H.; Sokolov, J.; Zhao, X.; Schwarz, S. A. *Europhys. Lett.* **1990**, *12*, 41.
(8) Hariharan, A.; Kumar, S. K.; Russell, T. P. *Macromolecules* **1991**, *24*, 4909.
(9) Schwarz, S. A.; Wilkens, B. J.; Pudensi, M. A. A.; Rafailovich, M. H.; Sokolov, J.; Zhao, X.; Zhao, W.; Zheng, X.; Russell, T. P.; Jones, R. A. L. *Mol. Phys.* **1992**, *76*, 937.
(10) Jones, R. A. L.; Kramer, E. J. *Polymer* **1993**, *34*, 115.
(11) Sakellariou, P. *Polymer* **1993**, *34*, 3408.
(12) Hong, P. P.; Boerio, F. J.; Smith, S. D. *Macromolecules* **1993**, *26*, 1460.
(13) Genzer, J.; Faldi, A.; Composto, R. J. *Phys. Rev. E* **1994**, *50*, 2373.
(14) Norton, L. J.; Kramer, E. J.; Bates, F. S.; Gehlsen, M. D.; Jones, R. A. L.; Karim, A.; Felcher, G. P.; Kleb, R. *Macromolecules* **1995**, *28*, 8621.
(15) Genzer, J.; Faldi, A.; Oslanec, R.; Composto, R. J. *Macromolecules* **1996**, *29*, 5438.
(16) Zink, F.; Kerle, T.; Klein, J. *Macromolecules* **1998**, *31*, 417.
(17) Hariharan, A.; Kumar, S. K.; Russell, T. P. *J. Chem. Phys.* **1993**, *98*, 4163.

(18) Tanaka, K.; Takahara, A.; Kajiyama, T. *Macromolecules* **1997**, *30*, 6626. (b) Tanaka, K.; Kajiyama, T.; Takahara, A.; Tasaki, S. *Macromolecules* **2002**, *35*, 4702.
(19) Hariharan, A.; Kumar, S. K.; Russell, T. P. *Macromolecules* **1990**, *23*, 3584. (b) Hariharan, A.; Kumar, S. K.; Russell, T. P. *J. Chem. Phys.* **1993**, *99*, 4041.
(20) Wattenbarger, M. R.; Chan, H. S.; Evans, D. F.; Bloomfield, V. A.; Dill, K. A. *J. Chem. Phys.* **1990**, *93*, 8343.
(21) Bitsanis, I. A.; ten Brinke, G. *J. Chem. Phys.* **1993**, *99*, 3100.
(22) Zhao, W.; Zhao, X.; Rafailovich, M. H.; Sokolov, J.; Composto, R. J.; Smith, S. D.; Satkowski, M.; Russell, T. P.; Dozier, W. D.; Mansfield, T. *Macromolecules* **1993**, *26*, 561.
(23) Elman, J. F.; Johs, B. D.; Long, T. E.; Koberstein, J. T. *Macromolecules* **1994**, *27*, 5341. (b) Koberstein, J. T. *MRS Bull.* **1996**, *21*, 19. (c) Mason, R.; Jalbert, C. A.; O'Rourke Muisener, P. A. V.; Koberstein, J. T.; Elman, J. F.; Long, T. E.; Gunesin, B. Z. *Adv. Colloid Interface Sci.* **2001**, *94*, 1.
(24) Tanaka, K.; Kawaguchi, D.; Yokoe, Y.; Kajiyama, T.; Takahara, A.; Tasaki, S. *Polymer* **2003**, *44*, 4171.
(25) Affrossman, S.; Hartshorne, M.; Kiff, T.; Pethrick, R. A.; Richards, R. W. *Macromolecules* **1994**, *27*, 1588.
(26) Schaub, T. F.; Kellogg, G. J.; Mayes, A. M.; Kulasekere, R.; Ankner, J. F.; Kaiser, H. *Macromolecules* **1996**, *29*, 3982.
(27) Kwei, T. K.; Nishi, T.; Roberts, R. F. *Macromolecules* **1974**, *7*, 667. (b) Nishi, T.; Kwei, T. K. *Polymer* **1975**, *16*, 285.
(28) Utracki, L. A. *Polymer Alloys and Blends, Thermodynamics and Rheology*; Carl Hanser Verlag: Munich, 1989.
(29) Pan, D. H. K.; Prest, W. M. *J. Appl. Phys.* **1985**, *58*, 2861.
(30) Bhatia, Q. S.; Pan, D. H.; Koberstein, J. T. *Macromolecules* **1988**, *21*, 2166.
(31) Dee, G. T.; Sauer, B. B. *Macromolecules* **1993**, *26*, 2771.
(32) Cowie, J. M. G.; Devlin, B. G.; McEwen, I. J. *Macromolecules* **1993**, *26*, 5628.
(33) Tanaka, K.; Yoon, J.-S.; Takahara, A.; Kajiyama, T. *Macromolecules* **1995**, *28*, 934.
(34) Lee, S.; Sung, C. S. P. *Macromolecules* **2001**, *34*, 599.
(35) Forrey, C.; Koberstein, J. T.; Pan, D. H. *Interface Sci.* **2003**, *11*, 211.
(36) Andrade, J. D. *Surface and Interfacial Aspects of Biomedical Polymers. Surface Chemistry and Physics*; Plenum: New York, 1985.
(37) Ashley, J. C. *IEEE Trans. Nucl. Sci.* **1980**, *NS-27*, 1454.
(38) Ebisawa, T.; Tasaki, S.; Otake, Y.; Funahashi, H.; Soyama, K.; Torikai, N.; Matsushita, Y. *Physica B* **1995**, *213−214*, 901.
(39) Welp, K. A.; Co, C. C.; Wool, R. P. *J. Neutron Res.* **1999**, *8*, 37.
(40) Russell, T. P. *Mater. Sci. Rep.* **1990**, *5*, 171.
(41) Stamm, M. In *Physics of Polymer Surfaces and Interfaces*; Sanchez, I. C., Ed.; Butterworth-Heinemann: Stoneham, 1992; p 163.
(42) Krausch, G.; Dai, C.-A.; Kramer, E. J.; Marko, J. F.; Bates, F. S. *Macromolecules* **1993**, *26*, 5566.
(43) Morita, H.; Kawakatsu, T.; Doi, M. *Macromolecules* **2001**, *34*, 8777.
(44) Ougizawa, T.; Dee, G. T.; Walsh, D. J. *Macromolecules* **1991**, *24*, 3834.
(45) Ballard, D. G. H.; Wignall, G. D.; Schelten, J. *Eur. Polym. J.* **1973**, *9*, 965.
(46) Beaucage, G.; Stein, R. S. *Macromolecules* **1993**, *26*, 1617.
(47) Beaucage, G.; Stein, R. S.; Koningsveld, R. *Macromolecules* **1993**, *26*, 1603.
(48) Schacht, P. A.; Koberstein, J. T. *Polymer* **2002**, *43*, 6527.
(49) Paynter, R. W. *Surf. Interface Anal.* **1981**, *3*, 186.
(50) We have tried to fit the experimental data with many models, and the ones presented in the inset were the best. However, we are not able to perfectly deny a possibility that a better model exists, although this does not mean that our discussion would alter depending on such models.

MA034117U